Development 124, 4615-4625 (1997)
Printed in Great Britain © The Company of Biologists Limited 1997
DEV3699

Differential H4 acetylation of paternal and maternal chromatin precedes DNA replication and differential transcriptional activity in pronuclei of 1-cell mouse embryos

Pierre G. Adenot, Yvan Mercier, Jean-Paul Renard and Eric M. Thompson*

Unité de Biologie du Développement, Institut National de la Recherche Agronomique, 78352 Jouy-en-Josas, France
*Author for correspondence (e-mail: thompson@biotec.jouy.inra.fr)

SUMMARY

In the mouse embryo, transcriptional activation begins during S/G_2 phase of the first cell cycle when paternal and maternal chromatin are still in separate nuclear entities within the same cytoplasm. At this time, the male pronucleus exhibits greater transcriptional activity than the female pronucleus. Since acetylation of histones in the nucleosome octamer exerts a regulatory influence on gene expression, we investigated changes in histone acetylation during the remodeling of paternal and maternal chromatin from sperm entry through to minor genome activation and mitosis. We found (1) neither mature sperm nor metaphase II maternal chromatin stained for hyperacetylated histone H4; (2) immediately following fertilization, hyperacetylated H4 was associated with paternal but not maternal chromatin while, in parthenogenetically activated oocytes, maternal chromatin became hyperacetylated; (3) in zygotes, differential levels and patterns of hyperacetylated H4 between male and female pronuclei persisted throughout most of G_1 with histone deacetylases and acetyltransferases already active at this time; (4) when transcriptional differences are observed in S/G_2, male and female pronuclei have equivalent levels of H4 hyperacetylation and DNA replication was not required to attain this equivalence and (5) in contrast to the lack of H4 hyperacetylation on gametic chromatin, chromosomes at the first mitosis showed distinct banding patterns of H4 hyperacetylation. These results suggest that sperm chromatin initially outcompetes maternal chromatin for the pool of hyperacetylated H4 in the oocyte, that hyperacetylated H4 participates in the process of histone-protamine exchange in the zygote, and that differences in H4 acetylation in male and female pronuclei during G_1 are translated across DNA replication to transcriptional differences in S/G_2. Prior to fertilization, neither paternal nor maternal chromatin show memory of H4 hyperacetylation patterns but, by the end of the first cell cycle, before major zygotic genome activation at the 2-cell stage, chromosomes already show hyperacetylated H4 banding patterns.

Key words: histone H4 acetylation, sperm, oocyte, cell cycle

INTRODUCTION

Complex control of spatially and temporally differential gene expression underlies the correct completion of a developmental program. Dynamic changes in chromatin structure play an essential role in this control by regulating both the access and three-dimensional juxtaposition of transcriptional activators and the basal transcriptional machinery to gene regulatory elements. It has long been suggested that modulation of acetylation of the N-terminal tails of the core histones is part of this regulation (Allfrey et al., 1964). Antibodies against specific isoforms of acetylated histone H4 reveal much higher levels of acetylation on the active mammalian X chromosome than on the inactive X (Jeppesen and Turner, 1993). Direct in vivo correlations between transcriptionally active genetic loci and histone acetylation have been established (Hebbes et al., 1988, 1994) and acetylation of histones facilitates transcription factor binding to nucleosomal DNA (Lee et al., 1993; Vettese-Dadey et al., 1996). Furthermore, the N-terminal tails of histones H3 and H4 have a critical role in the folding of higher order chromatin structures (Moore and Ausio, 1997). The recent identification of acetyltransferase activities in the transcriptional adapter Gcn5p (Brownell et al., 1996), and in p300/CBP (Ogryzko et al., 1996), TFIID (Mizzen et al., 1996) and PCAF (Yang et al., 1996) have established a direct link between histone acetylation and the transcriptional process. However, the chronology of core histone acetylation events with respect to transcription initiation remains unclear at present.

Modulation of core histone acetylation also appears to be intimately associated with activation of the zygotic genome (ZGA) at the onset of embryonic development. In *Xenopus* embryos, inhibition of histone deacetylases does not result in the accumulation of hyperacetylated histone H4 until ZGA at the mid-blastula transition (MBT) (Dimitrov et al., 1993). In the mouse embryo, where minor ZGA occurs in the late 1-cell embryo and major ZGA in the 2-cell embryo, distinct patterns of histone H4 acetylation are observed in the nucleus at these stages (Thompson et al., 1995; Worrad et al., 1995). Alteration of these patterns through inhibition of histone deacetylases has been shown to have an effect on the chromatin regulated

expression of the *HSP70.1* gene in cleavage-stage mouse embryos (Thompson et al., 1995). Of further note in the 1-cell mouse embryo is the differential transcriptional activity observed between female and male pronuclei. Reporter genes are preferentially expressed when microinjected into the male pronucleus (Ram and Shultz, 1993; Wiekowski et al., 1993) and, more generally, the male pronucleus incorporates higher levels of bromo UTP in transcription assays (Aoki et al., 1997). However, when histone deacetylases are inhibited in the 1-cell embryo, resulting in core histone hyperacetylation, reporter gene expression from the female pronucleus is equivalent to that observed in the male pronucleus (Wiekowski et al., 1993). Therefore, the different levels of transcription in the two pronuclei may have some basis in different chromatin structures.

The 1-cell embryo is a unique cell in that it is formed from two sets of chromatin that coexist as separate nuclear entities throughout the cell cycle. Initially, maternal chromatin is condensed in chromosomes with a nucleosomal structure whereas, in highly compacted sperm chromatin, most or all of the histones (species dependent, Bench et al., 1996) have been replaced by basic protamines. At this stage, both maternal and paternal chromatin appear to be transcriptionally inert. Upon sperm entry into the metaphase II oocyte, a series of biophysical and biochemical processes occur that affect both the cytoplasm and chromatin and lead to the formation of pronuclei (Perreault, 1992; Moos et al., 1996). Changes in chromatin structures involve the reduction of protamine disulfide bonds, the decondensation of sperm chromatin and the resumption of meiosis with the extrusion of an haploid set of maternal chromosomes. In the mouse, sperm protamines are progressively replaced by histones during the period between sperm entry and DNA replication, and this may be a prerequisite for entry into S phase (Nonchev and Tsanev, 1990). Decondensation of sperm chromatin is followed by a transient recondensation (Adenot et al., 1991), suggesting recompaction of sperm chromatin after nucleosomes have been formed. The male pronucleus forms shortly after the female pronucleus, and the pronuclei swell and migrate toward the center of the cell where they become apposed. The coordinated evolution of male and female pronuclei terminates with the condensation of chromosomes at syngamy to form an unique metaphase plate before the embryo cleaves into two cells. In contrast to subsequent embryonic cleavage stages, the G_1 phase of the first cell cycle in the mouse embryo is very long (9 hours), S phase lasts 6 hours, and G_2 is very short (1 hour) (Howlett, 1986).

In this study, we examined histone H4 acetylation in the remodeling of maternal and paternal chromatin in the 1-cell mouse embryo leading up to minor activation of the zygotic genome. Metaphase II chromatin of the oocyte and sperm chromatin showed undetectable levels of hyperacetylated histone H4. However, immediately upon sperm entry, hyperacetylated H4 was associated with sperm chromatin. Throughout most of G_1, the male pronucleus exhibited higher levels of hyperacetylated H4 than did the female pronucleus. During S phase and in G_2, levels of H4 hyperacetylation were equivalent in both pronuclei. DNA replication was not required to attain equivalent pronuclear acetylation and furthermore, it was possible to alter G_1 pronuclear acetylation levels in both male and female pronuclei through histone deacetylase inhibition. This suggests that different equilibria in deacetylase/acetyltransferase activities are maintained in G_1 female and male pronuclei. In contrast to metaphase II chromosomes, chromosomes at the first mitosis exhibited specific regions that were marked by hyperacetylated H4. Interestingly, at the point in time (S/G_2) where differential global transcriptional activities are observed between male and female pronuclei, levels of histone hyperacetylation were equivalent. This suggests that the observed transcriptional differences may reflect the differential evolution of acetylation in female and male pronuclei prior to DNA replication.

MATERIALS AND METHODS

Collection of embryos, oocytes and spermatozoa

Female C57/CBA mice, 6-8 weeks old, were superovulated with intraperitoneal injections of 5 IU of pregnant mare serum (PMS; Folligon, Intervet), followed 46-48 hours later with 5 IU human chorionic gonadotropin (hCG; Chlorulon, Intervet). 1-cell embryos were obtained from females that had been caged with C57/CBA males, either immediately after hCG injection, or at 13.5 hours post-hCG (phCG) (Adenot et al., 1991). To recover mature oocytes, superovulated females were killed at 16 hours phCG. Oocytes and embryos were incubated after collection in 0.5% hyaluronidase (Sigma) in PB1 for 1-2 minutes at 37°C to remove cumulus cells, washed extensively in PB1 and fixed. These procedures allowed us to obtain 1-cell embryos at all stages, including those prior to pronuclear formation and avoided in vitro culture in order to approach normal developmental conditions as closely as possible. Activated oocytes were obtained by exposure of MII oocytes to 8% ethanol in PB1 for 6 minutes. Sperm suspensions were prepared from caudae epididymides of adult C57/CBA males. Sperm were released in PB1 at 37°C, washed twice in 0.1 M PBS and incubated in 2 mM DTT in 0.1 M PBS for 20 minutes at 37°C. Sperm were then rinsed, resuspended in 20 μl PBS and spread on clean slides. Excess PBS was withdrawn and the sperm were fixed.

Immunofluorescence confocal microscopy

In mammalian somatic cells, histone H4 is acetylated in the order lysine 16, then lysine 8 or 12, and finally lysine 5 (Turner and Fellows, 1989). This is also the order in mouse embryonic stem cells (Keohane et al., 1996). Increased levels of transgene expression in early mouse embryos were also correlated with increased nuclear levels of histone H4 acetylated at lysine 5 (Thompson et al., 1995), and inhibition of histone deacetylases results in increased expression of endogenous genes in mouse 2-cell embryos (Aoki et al., 1997). Therefore, antibodies specific for histone H4 acetylated at lysine 5 will recognize the most highly acetylated isoforms and it was this antibody that was used in the experiments described here.

Sperm, oocytes and embryos were fixed as described (Thompson et al., 1995) except that alcohol fixation was for 30 minutes and paraformaldehyde fixation was performed for 20 minutes at room temperature without Triton X-100. Fixed cells were blocked in PBS containing 10% foetal calf serum (FCS) and 0.2% Triton X-100 for 30 minutes at 37°C. Subsequent manipulations were performed in PBS/2% FCS/0.1% Triton X-100. Nuclear antigens were detected by indirect immunofluorescence. Cells were incubated with mouse anti-pan-histone monoclonal antibodies (1:200 dilution; Boehringer) for 1 hour at 37°C, or with rabbit anti-histone H4 acetylated at lysine 5 polyclonal antibodies (H4-L5, 1:700 dilution) overnight at 4°C. They were then washed extensively before incubation for 1 hour at 37°C with FITC-conjugated second antibodies (1:400 dilution; Sigma). Chromatin was stained for 30 minutes with 10 μg/ml propidium iodide. Cells were mounted on well-slides in Moviol (Sigma) containing the same concentration of propidium iodide and

observed under a confocal laser scanning microscope (Carl Zeiss, CLSM 310).

Assessment of nuclear stage

To detect DNA replication, 1-cell embryos were incubated just after collection and removal of cumulus cells in 1 mM BrdU (Sigma) in PB1 for 15 minutes at 37°C, washed and immediately fixed in 2.5% paraformaldehyde containing 0.5 M NaOH for 15 minutes at room temperature. Immunofluorescence and observation were performed as above except that embryos were incubated for 1 hour at 37°C with mouse anti-BrdU monoclonal antibodies (1:500 dilution; Sigma) to detect DNA replication sites.

DNA replication and histone deacetylase inhibitors

To prevent DNA replication and retain pronuclei in G_1, 1-cell embryos were collected at 18 hours phCG, cultured for 4-5 hours in M16 medium at 37°C and fixed in the continuous presence of 10 μg/ml aphidicolin (Sigma). This concentration of aphidicolin completely blocked DNA replication in mouse embryos within 1 hour (Adenot et al., 1992).

To perturb histone H4 acetylation before pronuclear formation and/or before DNA replication, 1-cell embryos were collected 4 hours after the appearance of a vaginal plug in females that had been caged with males at 13.5 hours phCG. Embryos were cultured for 2 hours in M16 medium at 37°C and fixed in the continuous presence of 75 nM Trichostatin A (TSA), a reversible and specific inhibitor of histones deacetylases (Yoshida et al., 1990).

Quantitative analysis of fluorescence intensities

To classify pronuclear stages, the following parameters were measured for embryos mounted between the well-slide and the coverslip: the maximum section of the embryo, the maximum male and female pronuclear sections, the distance along the z-axis between pronuclear sections and the distance in the x-y plane between the centers of pronuclear sections. Confocal microscopy in the z-scan mode showed that mounted embryos were compressed and had the shape of a sphere without poles. This model was used to fit a calibration curve relating the height of the embryo to its maximum section. To determine the volume of an uncompressed embryo, it was assumed that the shape of the embryo, but not its volume, changed after mounting. As the level of compression was different for the whole embryo and for pronuclei, calibration curves were determined that related embryo height to the height of male and female pronuclei. A sigmoid curve was used to fit the calibration data. From the calculated embryo and pronuclear heights, and the parameters measured above, pronuclear surfaces and interpronuclear distances were corrected for compression. Data were normalized to an unfixed native embryo, minus zona pellucida, with a 65 μm diameter.

Image cytometric quantitative analysis of pronuclear H4-L5 fluorescence intensities in alcohol-fixed embryos was done by CLSM using a ×63 objective (numerical aperture 1.4) to reduce overlap of pronuclear fluorescence. To detect the total intensity of each pronucleus, a resolution on the z-axis ranging between 4 and 6 μm was obtained by opening the pinhole on the CLSM depending on the pronuclear stage and the level of embryo compression. The same pinhole was always used for both pronuclei within an embryo. Pronuclear fluorescence intensities were measured by manual outlining and thresholding, using CLSM software (Carl Zeiss), and were corrected for detector sensitivity. The H4-L5 fluorescence intensity of each pronucleus was divided by its propidium iodide fluorescence to correct for differences in the position of nuclei with respect to the objective lens. To determine the range in which two nuclei in the same embryo had similar normalized fluorescence intensities, 46-48 hour phCG 2-cell embryos in G_2 were alcohol fixed, immunolabelled for histones and the DNA stained as for 1-cell embryos. We used G_2 2-cell embryos for this calibration because the very short duration of G_2 in 1-cell embryos made accurate assessment of this chronological stage difficult. The data were expressed as the ratio of the normalized fluorescence intensity in the more strongly staining nucleus divided by the normalized fluorescence intensity in the more weakly fluorescent nucleus ($R_{max/min}$). The mean $R_{max/min}$ value of these G_2 nuclei was 1.13±0.104 (coefficient of variation, 9.3%; n=56), indicating that nuclei in the same embryo with a $R_{max/min}$ value lower than 1.4 had similar normalized fluorescence intensities (P<0.01).

Statistical analysis

Mean values of pronuclear surfaces and interpronuclear distances were compared using the Student's t-test. Chi-square analysis was used to compare the development of control versus TSA-treated embryos.

RESULTS

Changes in H4-L5 acetylation patterns from sperm entry to pronuclear formation

Before fertilization, no detectable labelling of histones was observed in sperm, whatever the level of chromatin decondensation (none to fully decondensed) obtained after incubation in 2 mM DTT (Fig. 1A,B). In mature oocytes, maternal chromatin contained histones (Fig. 1C,D) but did not show labelling for histone H4-L5 (Fig. 1E,H).

After fertilization, labelling was observed in sperm chromatin immediately upon sperm entry both for histones (not shown) and for histone H4-L5 (Fig. 2A,B). At this time, maternal chromatin was still in metaphase II and did not exhibit H4-L5 labelling. At anaphase II, histone H4-L5 staining of decondensing sperm chromatin was heterogeneous while maternal chromatin remained negative (Fig. 2C,D). During extrusion of the second polar body, H4-L5 staining was intense in decondensed sperm chromatin and, in some embryos (9/17), became homogeneous (Fig. 2E,F). A weak H4-L5 fluorescent signal was also observed in telophase II maternal chromatin (11/17). Following extrusion of the second polar body, sperm chromatin recondensed to an ovoid shape and nuclear membranes began to assemble (Adenot et al., 1991). Histone H4-L5 labelling of sperm chromatin remained intense both during recondensation and when the male pronucleus formed. The pattern was always homogeneous during sperm recondensation (Fig. 2G,H) but, during formation of the male pronucleus, a more intense labelling was visible at the nuclear periphery (Fig. 2I,J). Over this period, maternal chromatin remained weakly stained but a partial peripheral staining was sometimes observed (9/17) coincident with male pronuclear formation.

In distinct contrast to normal fertilization, parthenogenetic activation resulted in maternal chromatin showing an intense H4-L5 staining from meiosis resumption (Fig. 1F,I) to pronuclear formation (Fig. 1G,J).

Classification of pronuclear embryos in relation to biological events of the first cell cycle

1-cell embryos were classified into five pronuclear stages (PN1 to PN5) according to pronuclear size and location in the cytoplasm (Fig. 3). The distribution of PN stage embryos relative to phCG chronology is presented in Table 1. At 18 hours phCG, 60% of the embryos were in PN stages. However, when the presence of pronuclei was screened under the stereomicroscope at 18 hours phCG, only 25% of embryos (n=80)

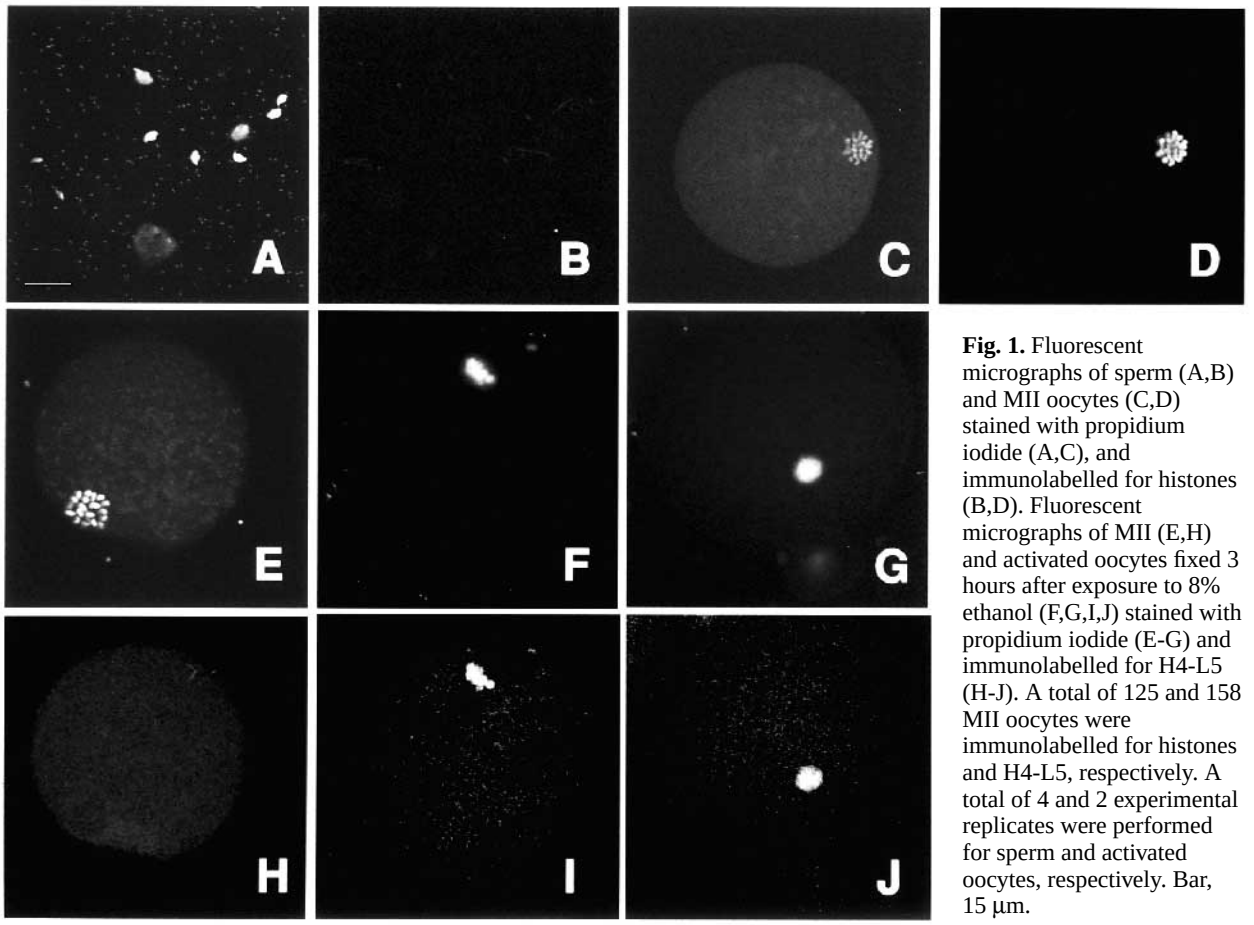

Fig. 1. Fluorescent micrographs of sperm (A,B) and MII oocytes (C,D) stained with propidium iodide (A,C), and immunolabelled for histones (B,D). Fluorescent micrographs of MII (E,H) and activated oocytes fixed 3 hours after exposure to 8% ethanol (F,G,I,J) stained with propidium iodide (E-G) and immunolabelled for H4-L5 (H-J). A total of 125 and 158 MII oocytes were immunolabelled for histones and H4-L5, respectively. A total of 4 and 2 experimental replicates were performed for sperm and activated oocytes, respectively. Bar, 15 μm.

showed visible pronuclei. After fixation and DNA staining, it was noted that embryos screened for visible pronuclei were in fact at the PN2 (25%) and PN3 stages (75%). At 21.5 hours phCG, large pronuclei (PN3-PN5) were observed in 50% of embryos. At 27.5 hours phCG, embryos began to enter mitosis and the proportion of PN5 stage embryos had attained its maximum. It cannot be excluded that the classification into PN stages may have been partially impaired by compression of embryos during mounting between the well-slide and the coverslip (see Materials and Methods). This would have increased pronuclear widths and simultaneously decreased apparent interpronuclear distance. In Table 2, pronuclear surfaces and interpronuclear distances measured from images of alcohol fixed embryos were corrected for compression. The calculated parameters were in agreement with our qualitative classification: the size of the male and female pronuclei in PN1, PN2 and PN3 embryos increased significantly (P<0.01), while the distance between pronuclei in PN3, PN4 and PN5 embryos decreased significantly (P<0.01).

The PN stages were then characterized with respect to DNA replication. Based on published timing for the beginning and end of DNA replication (Howlett, 1986), 1-cell embryos were exposed to a pulse of BrdU at 21, 22.5, 27.5 or 30 hours phCG and fixed immediately (Table 3). Although 14% of the embryos were already in S phase at 21 hours phCG, incorporation of BrdU was never detected in PN1 and PN2 embryos. From 21

Table 1. Chronological distribution of pronuclear stages in mouse embryos

	Time of fixation (hours phCG)*				
Stage	18.0 *n* (%)	21.5 *n* (%)	24.0 *n* (%)	27.5 *n* (%)	30.0 *n* (%)
<PNF	68 (40)	10 (5)	5 (2)	–	–
PN1	39 (23)	13 (6)	12 (6)	–	–
PN2	43 (25)	83 (39)	39 (19)	2 (1)	1 (1)
PN3	22 (13)	60 (28)	89 (43)	37 (25)	14 (9)
PN4	–	33 (16)	41 (20)	70 (47)	63 (41)
PN5	–	12 (6)	21 (10)	34 (23)	35 (23)
M	–	–	–	6 (4)	33 (21)
2-cell	–	–	–	–	9 (6)
Total	172 (100)	211 (100)	207 (100)	149 (100)	155 (100)

*17 to 21 females were killed at each time except at 30 hours phCG where 7 females were used. <PNF embryos were between sperm entry and pronuclear formation. M embryos were in syngamy or mitosis.

Table 2. Pronuclear surfaces and interpronuclear distances in PN stage embryos

Stage	*n*	S male (± s.d.) (μm^2)	S female (± s.d.) (μm^2)	Interpronuclear distance (± s.d.) (μm)
PN1	17	85±18	85±17	34.5±18.9
PN2	83	194±33	164±31	17.5±17.0
PN3	126	277±31	224±26	10.8±10.8
PN4	93	288±28	235±25	1.7±4.3
PN5	43	286±20	235±22	–2.5±2.0

S, pronuclear surface; s.d., standard deviation.

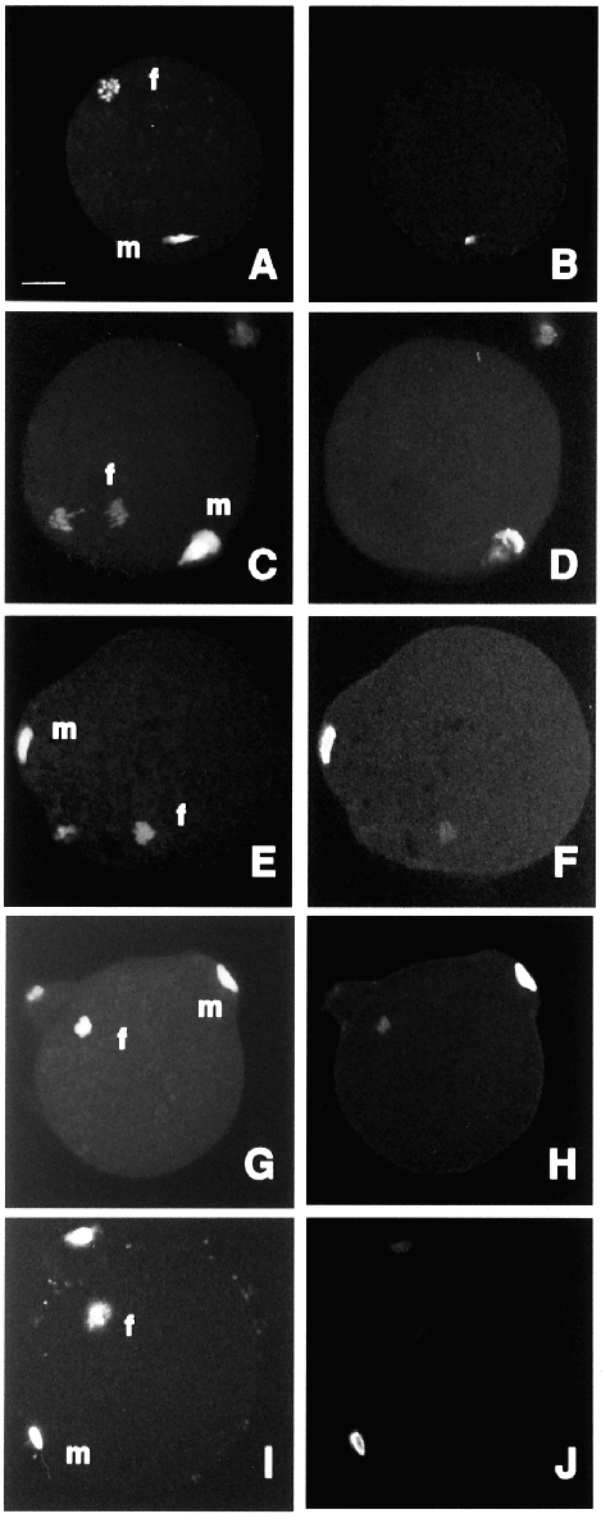

Fig. 2. Fluorescent micrographs of fertilized embryos just after sperm entry (A,B, *n*=2), during resumption of meiosis (anaphase II: C,D, *n*=4; telophase II: E,F, *n*=17), after second polar body extrusion (G,H, *n*=19), and during pronuclear formation (I,J, *n*=17). Column A-I, propidium iodide; column B-J, immunolabelling of histone H4-L5. m, male chromatin; f, female chromatin. Micrograph J was recorded at lower contrast. Bar, 14 μm.

Table 3. DNA replication in 1-cell embryos

	Time of BrdU incorporation (hours phCG)*			
Stage	21.0 BrdU+/*n*	22.5 BrdU+/*n*	27.5 BrdU+/*n*	30.0 BrdU+/*n*
PN1	0/5	0/3	–	–
PN2	0/19	0/22	–	–
PN3	5/16	14/52	19/22	7/11
PN4	1/2	4/4	31/45	25/58
PN5	0/1	1/2	4/22	3/29
Total	6/43	19/83	54/89	35/98
(% BrdU+)	(14)	(23)	(61)	(36)

*5 to 7 females were killed at each time.

to 30 hours phCG, incorporation was observed in PN3 and PN4 embryos, and in a few at the PN5 stage. Between 21 and 22.5 hours phCG, the proportion of PN3 embryos among all PN stages passed from 37% (16/43) to 62% (52/83), but the proportion of those PN3 embryos that were in S phase did not change, suggesting that DNA replication began when embryos were advanced in the PN3 stage. Between 27.5 and 30 hours phCG, the proportion of pronuclear embryos in S phase decreased considerably while the proportion of embryos with BrdU staining restricted to the female pronucleus increased from 22% (12/54) to 49% (17/35), indicating that the female pronucleus completed DNA replication after the male pronucleus. This asynchrony in replication between male and female pronuclei has also been independently observed in a recent study by Ferreira and Carmo-Fonseca (1997). These results show that PN1 and PN2 embryos were in G_1, PN3 and PN4 embryos were largely in S, and PN5 embryos were mostly in G_2.

Changes in H4-L5 acetylation patterns after pronuclear formation

The level and pattern of the pronuclear fluorescent signal depended on the fixation procedure. Paraformaldehyde fixation yielded a higher pronuclear fluorescent signal but also a higher background than alcohol fixation. Structure in very early stages including the MII oocyte and from sperm entry to PN2-PN3 pronuclei was better preserved by paraformaldehyde fixation, but alcohol fixation was superior in revealing the evolution of an increasingly filamentous chromatin structure from PN2 through to PN5 and syngamy (Fig. 4D,E) with heterogeneous H4-L5 patterns at these stages. A more intense H4-L5 signal was sometimes observed at the periphery of one or both pronuclei in 20% of PN2 embryos and 60% of PN3-PN5 embryos, but it was patchy and discontinuous (Fig. 5). Peripheral enrichment of H4-L5 frequently colocalized with chromatin-rich regions but was also found in peripheral zones that did not stain more densely for chromatin. No difference was observed in the number of female or male pronuclei showing peripheral staining. Peripheral staining was also seen when embryos were immunolabelled with anti-pan-histone antibodies but, in this case, the enriched staining was continuous around the periphery (not shown).

The H4-L5 fluorescence signal was low in the female pronucleus and intense in the male pronucleus at the PN1 stage, similar to the pattern observed before pronuclear formation. At the PN2 stage, mean fluorescence intensity in the female pronucleus markedly increased despite pronuclear swelling

Schematic representation of pronuclear stages in the mouse embryo

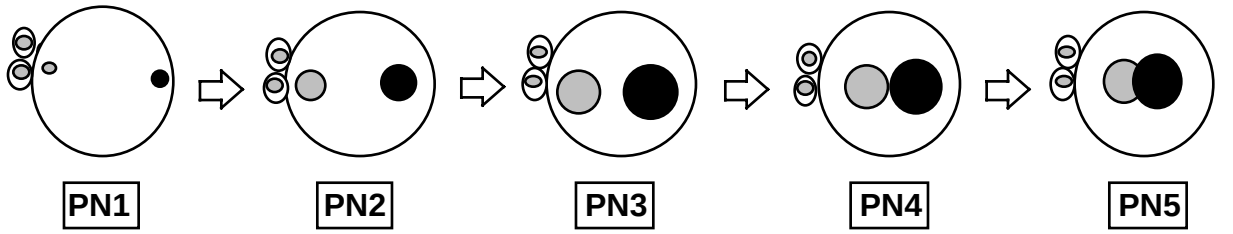

Fig. 3. Male and female chromatin are represented by dark and grey motifs, respectively. PN1, small pronuclei located at the periphery of the embryo. PN2, pronuclei increased in size and began migration towards the center of the embryo. PN3, large pronuclei migrated towards the center. PN4, large pronuclei were close to each other in the center of the embryo. PN5, large central pronuclei were apposed.

and, at the level of visual observation, became apparently similar to the male pronucleus. However, as male and female pronuclei swelled during the cell cycle and differed in size from each other, comparison of pronuclear levels of H4-L5 required quantitative analysis of fluorescence intensities. Quantitative differences between normalized male and female pronuclear H4-L5 fluorescence intensities in embryos fixed at 21.5 and 27.5 hours phCG are shown in Table 4. The data are presented as the ratio of the more intensely staining pronucleus to the least intensely staining nucleus. At the PN1 stage, the male pronucleus showed a normalized H4-L5 fluorescence intensity 3-fold to 22-fold greater than the female pronucleus (mean 7.2±6.0). At the PN2 stage, this ratio decreased but the majority (74%) still showed a higher normalized H4-L5 fluorescence intensity in the male pronucleus. From the PN3 stage on, most embryos had the same H4-L5 intensity in both pronuclei (83%, 84% and 92% in PN3, PN4 and PN5 embryos, respectively), the remaining embryos showing higher staining in the male pronucleus**,** with the exception of one PN4 embryo.

The entry of embryos into mitosis began by the condensation of both pronuclei, before they mixed to form a single metaphase plate. During pronuclear condensation (Fig. 4), the H4-L5 pattern was heterogenous in both pronuclei; intense labelling was found on some regions of condensing chromosomes, generally at the periphery of the pronucleus, both for the paternal and the maternal genome. When chromosomes were arranged on the metaphase plate, they still exhibited H4-L5 staining, with an heterogeneous pattern along their arms and therefore differed very significantly from meiotic chromosomes that were not labelled**.**

Evolution of pronuclear H4-L5 levels occurs before DNA replication

The data in Table 4 show that 26% of PN2 and 83% of PN3 embryos had the same H4-L5 fluorescence intensity in both pronuclei. However, PN2 embryos did not show any detectable amounts of DNA replication and replication began in embryos that were advanced into the PN3 stage, suggesting that DNA

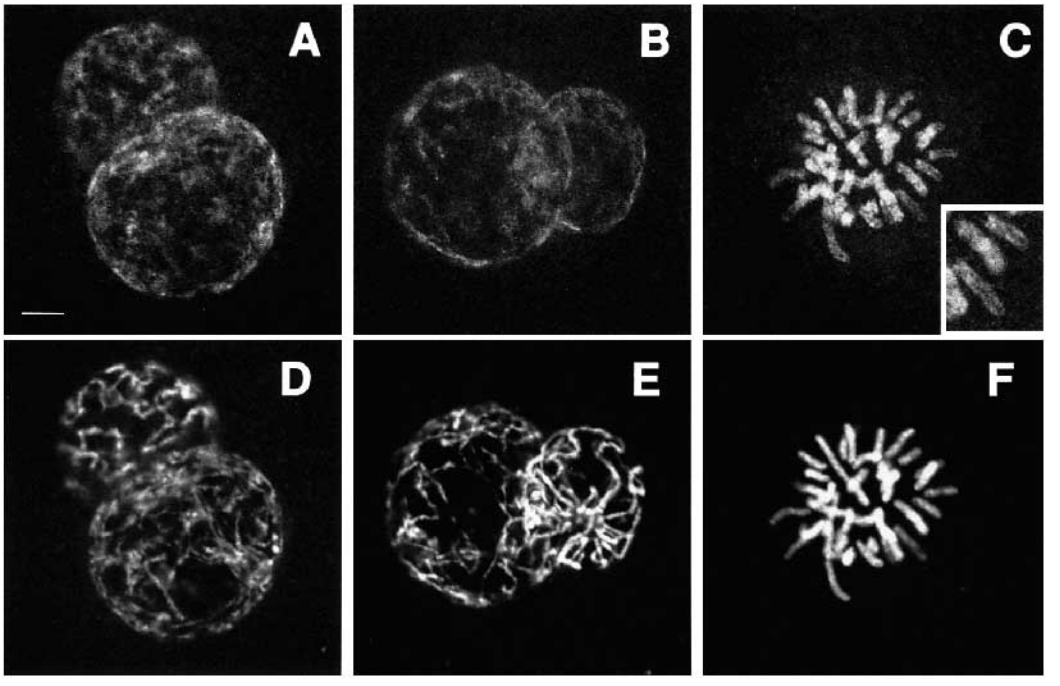

Fig. 4. Fluorescent micrographs of fertilized embryos at syngamy (A,B, D,E), and mitosis (C,F). (A-C) Immunolabelling of histone H4-L5. (D-F) Propidium iodide. The inset in C shows the H4-L5 banding observed on chromosomes. Bar, 5 μm.

Table 4. Ratio of H4-L5 levels in male and female pronuclei

*$R_{max/min}$	PN1 *n* (%)	PN2 *n* (%)	PN3 *n* (%)	PN4 *n* (%)	PN5 *n* (%)
†1.0<x<1.2	–	2 (5)	23 (58)	35 (67)	16 (70)
†1.2<x<1.4	–	9 (21)	10 (25)	9 (17)	5 (22)
1.4<x<1.6	–	16 (37)	4 (10)	3 (6)	–
1.6<x<1.8	–	4 (9)	2 (5.0)	2 (4)	2 (9)
1.8<x<2.0	–	4 (9)	1 (2.5)	2 (4)	–
2.0<x<2.2	–	–	–	–	–
2.2<x<2.4	–	1 (2)	–	–	–
2.4<x<2.6	–	2 (5)	–	–	–
2.6<x<2.8	–	1 (2)	–	–	–
2.8<x<3.0	1 (9)	–	–	1 (2)‡	–
3.0<x	10 (91)	4 (9)	–	–	–
Total	11 (100)	43 (100)	40 (100)	52 (100)	23 (100)

*Within a 1-cell embryo, $R_{max/min}$ is the ratio of the normalized fluorescence intensity of H4-L5 in the more strongly staining pronucleus divided by the normalized intensity in the more weakly staining pronucleus ($[I_{h4\text{-}L5}/I_{DNA}]_{max}/[I_{H4\text{-}L5}/I_{DNA}]_{min}$).

†The interval in which the two pronuclei had a statistically equivalent normalized fluorescence intensity (see Materials and Methods). Where significant differences were observed, the male pronucleus always showed higher H4-L5 levels than the female pronucleus with the exception of the denoted (‡) embryo.

Table 5. Effect of blocking DNA replication on pronuclear H4-L5 levels

*$R_{max/min}$	PN1 *n* (%)	PN2 *n* (%)	PN3 *n* (%)	PN4 *n* (%)	PN5 *n* (%)
†1.0<x<1.2	–	2 (15)	18 (45)	13 (68)	6 (38)
†1.2<x<1.4	–	3 (23)	11 (28)	4 (21)	6 (38)
1.4<x<1.6	–	2 (15)	6 (15)	2 (11)	4 (25)
1.6<x<1.8	–	3 (23)	3 (8)	–	–
1.8<x<2.0	–	1 (8)	–	–	–
2.0<x<2.2	–	–	2 (5)	–	–
2.2<x<2.4	–	–	–	–	–
2.4<x<2.6	–	1 (8)	–	–	–
2.6<x<2.8	1 (100)	1 (8)	–	–	–
2.8<x<3.0	–	–	–	–	–
3.0<x	–	–	–	–	–
Total	1 (100)	13 (100)	40 (100)	19 (100)	16 (100)

*$R_{max/min} = I_{h4\text{-}L5}/I_{DNA}]_{max}/[I_{H4\text{-}L5}/I_{DNA}]_{min}$).

†The interval in which the two pronuclei had a statistically equivalent normalized fluorescence intensity (see Table 4). Below the dashed line, male pronuclei always had significantly higher H4-L5 staining than female pronuclei.

replication was not involved in attaining equivalent pronuclear H4-L5 levels. To test this hypothesis, 1-cell embryos were collected at 18 hours phCG and incubated with aphidicolin to prevent DNA replication up to their fixation at 22.5-23 hours phCG (Table 5). At this time, only one PN1 embryo was found among 89 specimens, and its normalized H4-L5 fluorescence intensity was 2.7 times higher in the male than in the female pronucleus. At the PN2 stage, a majority (62%) still showed a higher normalized H4-L5 fluorescence intensity in the male pronucleus. From the PN3 stage on, most embryos had pronuclei with the same normalized intensity (73%, 90% and 75% in PN3, PN4 and PN5 embryos, respectively). The differences between normalized pronuclear fluorescence intensities observed in aphidicolin-treated embryos were distributed similarly to those observed in untreated embryos (Table 4), indicating that the occurrence of an equivalent level of H4-L5 in both pronuclei did not depend on DNA replication.

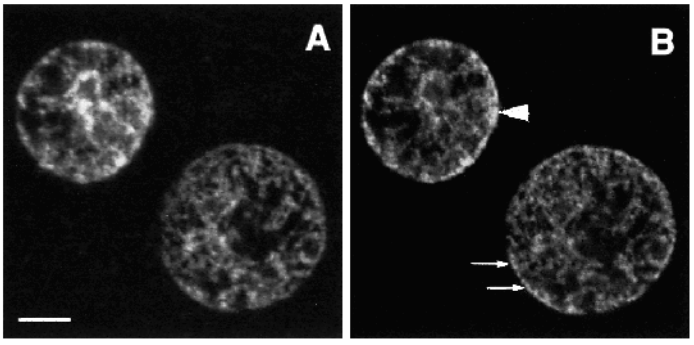

Fig. 5. Discontinuous peripheral enrichment of H4-L5 staining in female and male pronuclei. (A) Propidium iodide staining; (B) H4-L5 staining. Increased peripheral H4-L5 staining was frequently colocalized with areas enriched in chromatin (arrowhead) but was also found in peripheral zones, which did not exhibit increased chromatin density (arrows). Bar, 6 μm.

Transient histone deacetylase inhibition alters H4-L5 patterns but does not affect preimplantation development

The results presented above demonstrate a differential evolution of histone H4 acetylation levels in male and female pronuclei which preceded and were independent of DNA replication. We next asked if it was possible to alter these differential levels of acetylation and whether transient alterations at specific stages of the cell cycle in the 1-cell embryo had subsequent effects on preimplantation development.

Embryos treated with trichostatin A (TSA) always exhibited higher H4-L5 fluorescent signals than untreated embryos (Fig. 6), indicating that regulated acetylation/deacetylation activities are already present before pronuclear formation and DNA replication. Recondensing sperm chromatin was much more highly stained in TSA-treated embryos than was maternal chromatin. There was an intense peripheral staining around sperm chromatin while telophase II female chromatin exhibited a homogenous H4-L5 pattern in the presence of TSA. At the PN1 stage, the H4-L5 patterns and intensities were similar to what was observed before pronuclear formation. At the PN2 stage H4-L5 fluorescence intensity in female pronuclei increased. From this stage on, peripheral staining around the male pronucleus became discontinuous (in 5/12 PN2 and 14/17 PN3 embryos) or disappeared (in 2/17 PN3 embryos), while a discontinuous peripheral staining became visible around the female pronucleus (in 7/12 PN2 and 16/17 PN3 embryos).

Thus, inhibition of histone deacetylases prior to DNA replication resulted in hyperacetylation of both male and female chromatin but differences remained in acetylation patterns between the two pronuclei. Increased staining at the nuclear periphery in PN1 and PN2 pronuclei was restricted to the male pronucleus and only became evident as a discontinuous peripheral staining in female pronuclei of PN2-PN3 embryos.

To determine whether these transient alterations in H4-L5 acetylation patterns before or during the minor activation of the zygotic genome could influence preimplantation development, embryos were cultured for 2 hours in the presence of TSA at 17.5 (G_1), 25 (S), or 27.5 (G_2) hours phCG, before they were

extensively rinsed and returned to normal culture (Table 6). TSA treatment did not affect embryo development when it occurred between 17.5 and 19.5 or 25 and 27 hours phCG, while a low but significant (P<0.01) decrease of the blastocyst rate was obtained when TSA was added at 27.5 hours pHCG. Thus a transient increase in histone acetylation during the first cell cycle had little to no consequences for preimplantation development of mouse embryos.

DISCUSSION

As well as being stocked with the maternal mRNAs and proteins required to direct the earliest phases of development up to the activation of the zygotic genome, the oocyte is also a specialized cell with considerable chromatin remodeling capacity. A striking example of this is the reorganization of the paternal genome, which arrives packaged in basic protamines, is decondensed and then repackaged into nucleosomes containing histone octamers. Several in vitro studies using *Xenopus* oocyte extracts have shown that nucleosome assembly and sperm decondensation are both mediated by nucleoplasmin (Philpott and Leno, 1992). In the same model system, nucleoplasmin plays an important role in the remodeling of somatic nuclei through the selective removal of linker histones H1 and H1°, allowing their replacement by the embryonic linker histone B4 (Dimitrov and Wolffe, 1996). The extent to which the oocyte can remodel chromatin and reprogram appropriate patterns of developmental gene expression has perhaps been most provocatively demonstrated in the cloning of a sheep from an adult somatic cell (Wilmut et al., 1997).

One goal of the chromatin remodeling carried out in the 1-cell embryo is to prepare the zygotic genome for correctly regulated transcriptional activity. In the mouse embryo, this is a particularly urgent problem as major ZGA occurs at the 2-cell stage. The importance of core histone acetylation as an important regulatory parameter for transcription in a chromatin context lead us to examine histone H4 acetylation during the remodeling of paternal and maternal chromatin in the 1-cell mouse embryo leading up to minor ZGA, and how the greater transcriptional activity of the male compared to the female pronucleus might be related to differences in the progression of histone H4 acetylation patterns.

Chromatin remodeling in the early zygote

Late in spermatogenesis, at the mid-spermatid stage, hyperacetylation of histone H4 facilitates the replacement of histones by protamines (Christensen et al., 1984; Grimes and Smart, 1985), by promoting a relaxed nucleosomal structure leading to nucleosome disassembly and competitive protamine DNA binding (Oliva et al., 1987). Although mammalian species such as the human (Gatewood et al., 1990) retain some histones in the mature sperm, including acetylated isoforms of H4, histones are at undetectable levels in mouse sperm (O'Brien and Bellvé, 1980). In agreement, we detected no H4-L5 in mature mouse sperm prior to fertilization. In the mouse oocyte, it has been calculated from rates of histone H4 synthesis in oocytes, that the pool of H4 is sufficient to allow 2 to 3 rounds of DNA replication (Wassarman and Mrozak, 1981), and newly synthesized histones, both in unfertilized oocytes and in zygotes, rapidly undergo post-translational modifications with part of the pool becoming mono-, di- or tri-acetylated (Kaye and Wales, 1981; Kaye and Church, 1983). Therefore, it is interesting that, while maternal chromatin at metaphase II in unfertilized oocytes, or in zygotes, had very low levels of H4-L5, sperm chromatin

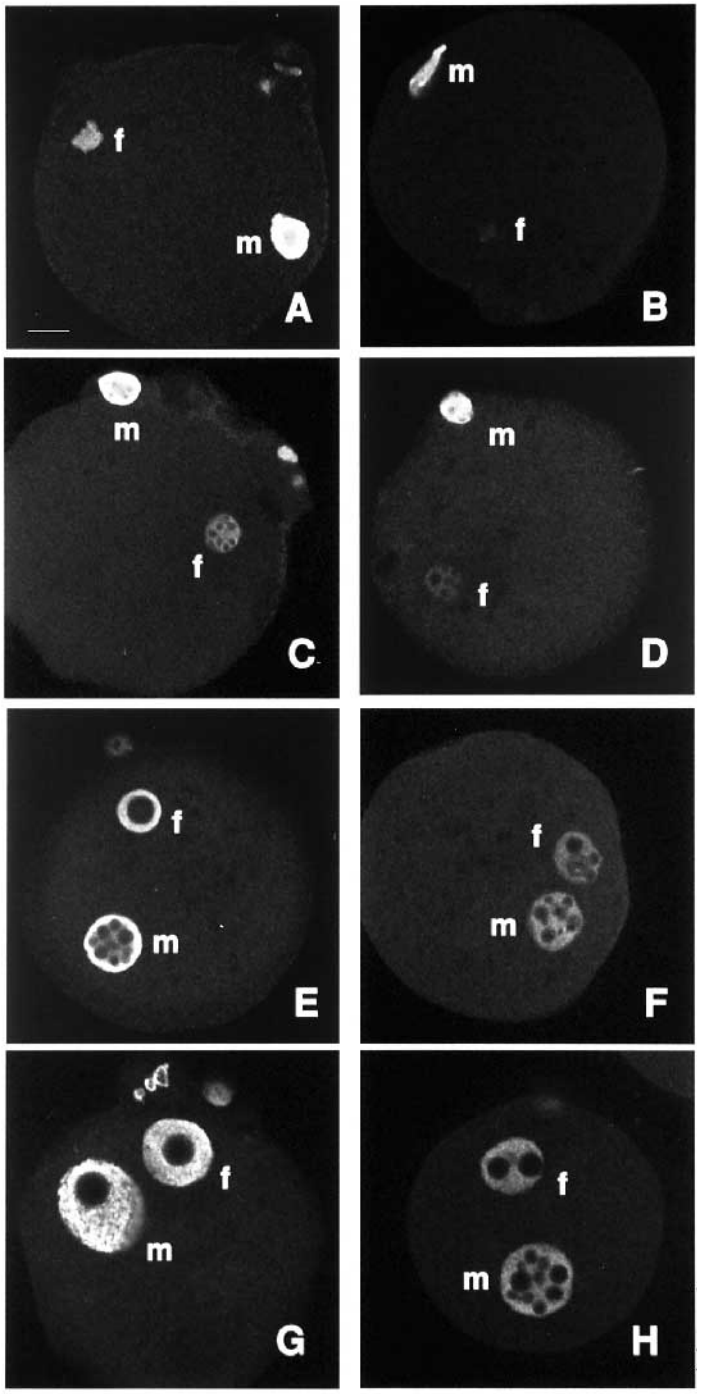

Fig. 6. Fluorescent micrographs of fertilized embryos cultured for 2 hours with (column A-G), or without (column B-H), 75 nM TSA until paraformaldehyde fixation and immunolabelling for histone H4-L5. Embryos were between second polar body extrusion and pronuclear formation (A,B), at PN1 (C,D), PN2 (E,F) and PN3 stages (G,H). Two replicates were done. Bar, 10 μm.

Table 6. Effect of TSA on in vitro development of embryos

Time*	TSA	Developmental stage		
		1-cell†	2-Cell (%)‡	Blastocyst (%)‡
17.5-19.5	+	107	104 (97)	87 (81)
	–	57	55 (96)	42 (74)
25-27	+	269	243 (90)	213 (79)
	–	107	98 (92)	90 (84)
27.5-29.5	+	243	225 (93)	192 (79)
	–	134	133 (99)	122 (91)

*Hours post hCG.
†The number of embryos obtained from 14 to 20 females at each time interval.
‡Percentage of initial 1-cell embryos.

showed intense H4-L5 fluorescent staining immediately following entry into the oocyte. In contrast, in activated oocytes, in the absence of sperm chromatin, we observed that maternal chromatin became markedly stained for H4-L5. This difference in maternal chromatin under conditions of parthenogenetic activation versus normal fertilization raises the question as to what role early acquisition of different functional states of parental chromatin might play in imprinting mechanisms (Solter, 1988). Thus, it seems that association of hyperacetylated H4 with DNA is a major event that occurs upon fertilization or artificial activation of the oocyte and that, during normal fertilization, paternal chromatin outcompetes maternal chromatin for hyperacetylated H4. This also suggests that, as was observed for packaging sperm DNA by replacing histones with protamines, acetylated H4 is also important in the reverse process in the zygote, of replacing sperm protamines with histones. Protamines appear to disappear completely in the mouse zygote before replication, with paternal chromatin attaining a nucleosomal structure characteristic of a somatic nucleus (Nonchev and Tsanev, 1990).

Transcriptional activity in male and female pronuclei

The male pronucleus is more transcriptionally active than the female pronucleus as determined by general BrUTP incorporation (Aoki et al., 1997) and increased reporter gene expression following pronuclear microinjection (Ram and Schultz, 1993; Wiekowski et al., 1993). The male pronucleus also appears to contain higher concentrations of the transcription factors Sp1 and TBP than the female pronucleus (Worrad et al., 1994). However, reporter gene expression from the female pronucleus is equivalent to the male pronucleus when zygotes are incubated in butyrate (Wiekowski et al., 1993) and BrUTP incorporation into parthenogenetic eggs is equivalent to that observed in fertilized zygotes (Aoki et al., 1997). Thus, the female pronucleus does not seem to be inherently deficient in transcriptional capacity and the fact that butyrate treatment results in core histone hyperacetylation suggests that differences in chromatin structure of the two pronuclei underly the differences observed in transcriptional activity.

Paradoxically, the times at which reporter constructs are microinjected into pronuclei, and when differences in transcription are detected (i.e. in S and G_2) correspond to periods when levels of histone H4 hyperacetylation in male and female pronuclei were equivalent. What differed between male and female pronuclei were their respective histories of histone hyperacetylation during the first cell cycle. The replacement of protamines by histones during sperm decondensation has been proposed to provide an opportunity for the binding of transcription factors to paternal DNA (Aoki et al., 1997), thus accounting for the transcriptional differences. This fails to explain why female pronuclei in parthenogenetic eggs show higher levels of transcription than female pronuclei in zygotes, as in neither case is there a protamine-histone exchange on maternal chromatin. Alternatively, it could be argued that, in the absence of the male pronucleus, the female pronucleus accumulates higher levels of transcription factors. This, though, would still not explain the observed increase in acetylation levels of parthenogenetic female chromatin, which had already been packaged in histone octamer nucleosomes. However, immediately following sperm entry into the oocyte, hyperacetylated histones were associated with paternal, and not with maternal, chromatin. This difference was reduced throughout most of G_1 until just prior to DNA replication when equivalence was attained. These differences seem to arise from (1) more efficient initial competition of paternal chromatin for the maternal pool of hyperacetylated H4, and (2) maintenance of different histone acetyltransferase/histone deacetylase activity equilibria in female and male pronuclei. Evidence for the first point comes from the observation that, in activated eggs, maternal chromatin becomes rapidly hyperacetylated in the absence of paternal chromatin. That enzymatic activities for modifying histone acetylation do exist in male and female pronuclei was confirmed by the observation that inhibition of histone deacetylase activity increased H4 acetylation in G_1 in both male and female pronuclei. Not only did levels of H4 acetylation differ between male and female pronuclei, but so did the distribution of H4-L5 within the pronuclei. During pronuclear formation, paternal chromatin showed an intense peripheral staining whereas maternal chromatin had even staining. When histone deacetylase activities were inhibited, strong peripheral staining persisted in the male pronucleus of PN1 and PN2 embryos and became discontinuous in PN3 embryos. Under the same conditions, the female pronucleus showed a weak, discontinuous peripheral staining in some PN2 and most PN3 embryos. We propose that it is these initial differences in histone acetylation during G_1 that result in preferential recruitment of transcription factors into the male pronucleus and the establishment of a chromatin structure prior to DNA replication, which leads to higher transcriptional activity in the paternal pronucleus during S/G_2.

Cell memory and setting up zygotic gene expression

It has been proposed that patterns of histone acetylation might be a mechanism for maintaining cell memory through mitosis (Jeppesen, 1997). Patterns of gene expression need to be reinstated after passage of the DNA replication fork in S phase and following general transcriptional repression during mitosis. Existing nucleosomal acetylation states can be transmitted to newly assembled chromatin after replication (Perry et al., 1993), and hyperacetylated regions of chromosomes at metaphase appear in the same chromatin domains during interphase (Jeppesen and Turner, 1993; Surrallés et al., 1996). Transcription factors that are displaced by the replication fork may compete with histones for assembly onto new DNA but, at mitosis, many transcription factors are dissociated from chromatin (Martinez-Balbas et al., 1995) though some, such as

AP-2 and the serum response factor, p67 srf, do remain attached. While this may exclude transcription factor binding as the means of propagating cell memory through mitosis, it has been noted that 10-20% of the cellular content of the general transcription factor TFIID remains attached to mitotic chromosomes (Segil et al., 1996) and this may serve as a basal marker for transcriptional activation that could be reamplified by subsequent attachment of other transcription factors as the nucleus reforms. However, as higher levels of histone acetylation seem to be correlated with regions of chromatin that are active or potentially active for transcription (Hebbes et al., 1988, 1994), the maintenance of acetylation both through replication and mitosis, would provide a mechanism by which transcription could be reactivated both following replication, and in G_1 after mitosis. These two mechanisms are not mutually exclusive and could act synergistically.

Our results support the idea that histone acetylation may be involved in cell memory but suggest that some refinement is necessary. Differences in histone acetylation of male and female pronuclei during G_1 of the 1-cell stage were translated across the first cycle of DNA replication to higher transcriptional levels in the male pronucleus. We also noted that, at the first mitosis, the chromosomes showed banding patterns of histone hyperacetylation. This indicates that regions of the genome are already marked prior to major ZGA at the 2-cell stage. In fact, specific global patterns of H4 acetylation persist in interphase nuclei through to the 8-cell stage (Thompson et al., 1995). While these characteristics reflect in general terms what is seen in somatic cells, the 1-cell zygote is unique in that, at the beginning of the cell cycle, neither paternal nor maternal chromatin show any patterns of histone hyperacetylation. What then are the cell memory mechanisms that lead from gametic chromatin to the specific patterns of gene expression seen in the early embryo? Are they sequence encoded or do some of the proteins involved in chromatin remodeling in the early zygote provide the link to the distinct patterns of H4 acetylation observed during the first cell cycle?

Establishing histone acetylation patterns in the 1-cell embryo

The modification of histone H4 acetylation patterns in pronuclei through inhibition of histone deacetylase activity by TSA demonstrated that acetyltransferases and deacetylases are active as early as G_1 in the 1-cell embryo. It is known that, in early *Xenopus* embryos, inhibition of histone deacetylation by TSA does not affect development until gastrulation (Almouzni et al., 1994). If inhibition of histone deacetylation is maintained in preimplantation mouse embryos through continuous culture in TSA, development is blocked after one or two cell divisions (Thompson, unpublished results). However, embryos that underwent 2 hour transient perturbation of acetylation patterns via histone deacetylase inhibition in G_1, S or G_2 of the first cell cycle were able to complete preimplantation development essentially as well as control embryos. Taken together, these results suggest that, in the mouse embryo, the ability to modulate acetylation levels is critical for correct development during preimplantation cleavage phases and that the early embryo has the capacity to rapidly compensate for deviations from normal levels of acetylation. With the recent cloning of a number of histone acetyltransferases (Brownell et al., 1996; Mizzen et al., 1996; Ogryzko et al., 1996; Yang et al., 1996) and deacetylases (Rundlett et al., 1996), it should now become possible to examine whether specific nuclear compartmentalization of these modifying enzymes are involved in establishing the acetylation patterns observed during early mouse embryogenesis. Specific inhibitors of histone acetyltransferases would also aid in defining more clearly the role of acetylated core histone acetylation in the processes of chromatin remodeling and preparation for ZGA, two essential activities in the 1-cell embryo.

We thank Dr Bryan Turner, University of Birmingham, for the antibody against histone H4 acetylated at lysine 5, and Bertrand Nicolas, INRA, for help with the photomicrographs.

REFERENCES

Adenot, P. G., Szöllösi, M. S., Geze, M., Renard, J. P. and Debey, P. (1991). Dynamics of paternal chromatin changes in live one-cell mouse embryo after natural fertilization. *Mol. Reprod. Dev.* **28**, 23-34.

Adenot, P. G., Corteggiani, E., Geze, M., Bezombes, D. and Debey, P. (1992). The DNA content of mouse two-cell embryos can be measured by microfluorimetric image analysis under conditions of cell viability. *J. Fluorescence* **2**, 181-190.

Allfrey, V. G., Faulkner, R. and Mirsky, A. E. (1964). Acetylation and methylation of histones and their possible role in the regulation of RNA synthesis. *Proc. Natl. Acad. Sci. USA* **51**, 786-794.

Almouzni, G., Khochbin, S., Dimitrov, S., and Wolffe, A. P. (1994). Histone acetylation influences both gene expression and development of *Xenopus laevis*. *Dev. Biol.* **165,** 654-669.

Aoki, F., Worrad, D. M. and Schultz, R. M. (1997). Regulation of transcriptional activity during the first and second cell cycles in the preimplantation mouse embryo. *Dev. Biol.* **181**, 296-307.

Bench, G. S., Friz, A. M., Corzett, M. H., Morse, D. H. and Balhorn, R. (1996). DNA and total protamine masses in individual sperm from fertile mammalian subjects. *Cytometry* **23**, 263-271.

Brownell, J. E., Zhou, J., Ranalli, T., Kobayashi, R., Edmondson, D. G., Roth, S. Y. and Allis, C. D. (1996). *Tetrahymena* histone acetyltransferase A: a homolog to yeast Gcn5p linking histone acetylation to gene activation. *Cell* **84**, 843-851.

Christensen, M. E., Rattner, J. B. and Dixon, G. H. (1984). Hyperacetylation of histone H4 promotes chromatin decondensation prior to histone replacement by protamines during spermatogenesis in rainbow trout. *Nucl. Acid Res.* **12**, 4575-4592.

Dimitrov, S., Almouzni, G., Dasso, M. and Wolffe, A. P. (1993). Chromatin transitions during early *Xenopus* embryogenesis: changes in histone-H4 acetylation and in linker histone type. *Dev. Biol.* **160**, 214-227.

Dimitrov, S. and Wolffe, A. P. (1996). Remodeling somatic nuclei in *Xenopus laevis* egg extracts: Molecular mechanisms for the selective release of histones H1 and H1° from chromatin and the acquisition of transcriptional competence. *EMBO J.* **15**, 5897-5906.

Ferreira, J. and Carmo-Fonseca, M. (1997). Genome replication in early mouse embryos follows a defined temporal and spatial order. *J. Cell Sci.* **110**, 889-897.

Gatewood, J. M., Cook, G. R., Balhorn, R., Schmid, C. W. and Bradbury, E. M. (1990). Isolation of four core histones from human sperm chromatin representing a minor subset of somatic histones. *J. Biol. Chem.* **265**, 20662-20666.

Grimes, S. R. and Smart, P. G. (1985). Changes in the structural organization of chromatin during spermatogenesis in the rat. *Biochim. Biophys. Acta* **824**, 128-139.

Hebbes T. R., Thorne, A. W. and Crane-Robinson, C. (1988). A direct link between core histone acetylation and transcriptionally active chromatin. *EMBO J.* **7**, 1395-1402.

Hebbes T. R., Clayton A.L., Thorne, A.W. and Crane-Robinson, C. (1994). Core histone hyperacetylation co-maps with generalized DNAse I sensitivity in the chicken *B*-globin chromosomal domain. *EMBO J.* **13**, 1823-1830.

Howlett, S. K. (1986). The effect of inhibiting DNA replication in the one-cell mouse embryo. *Roux's Arch. Dev. Biol.* **195**, 499-505.

Jeppesen, P. and Turner, B. M. (1993). The inactive X chromosome in female

mammals is distinguished by a lack of histone H4 acetylation, a cytogenetic marker for gene expression. *Cell* **74**, 281-289.

Jeppesen, P. (1997). Histone acetylation: A possible mechanism for the inheritance of cell memory at mitosis. *BioEssays* **19**, 67-74.

Kaye, P. L. and Wales, R. G. (1981). Histones synthesis in preimplantation mouse embryos. *J. Exp. Zool.* **216**, 453-459.

Kaye, P. L. and Church, R. B. (1983). Uncoordinated synthesis of histones and DNA by mouse eggs and preimplantation embryos. *J. Exp. Zool.* **226**, 231-237.

Keohane, A. M., O'Neill, L. P., Belyaev, N. D., Lavender, J. S. and Turner, B. M. (1996). X-inactivation and histone H4 acetylation in embryonic stem cells. *Dev. Biol.* **180**, 618-630.

Lee, D. Y., Hayes, J. J., Pruss, D. and Wolffe, A. P. (1993). A positive role for histone acetylation in transcription factor access to nucleosomal DNA. *Cell* **72**, 73-84.

Martinez-Balbas, M. A., Dey, A., Rabindran, S. K., Ozato, K. and Wu, C. (1995). Displacement of sequence-specific transcription factors from mitotic chromatin. *Cell* **83**, 29-38.

Mizzen, C. A., Yang, X.-J., Kokubo, T., Brownell, J. E., Bannister, A. J., Owen-Hughes, T., Workman, J., Wang, L., Berger, S. L., Kouzarides, T., Nakatani, Y. and Allis, C. D. (1996). The $TAF_{II}250$ subunit of TFIID has histone acetyltransferase activity. *Cell* **87**, 1261-1270.

Moore, S. C. and Ausio, J. (1997). Major role of the histones H3-H4 in the folding of the chromatin fiber. *Biochem. Biophys. Res. Commun.* **230**, 136-139.

Moos, J., Xu, Z., Schultz, R. M. and Kopf, G. S. (1996). Regulation of nuclear envelope assembly/disassembly by MAP kinase. *Dev. Biol.* **175**, 358-361.

Nonchev, S. and Tsanev, R. (1990). Protamine-histone replacement and DNA replication in the male mouse pronucleus. *Mol. Reprod. Dev.* **25**, 72-76.

O'Brien, D. A. and Bellvé, A. R. (1980). Protein constituents of the mouse spermatozoon. I. An electrophoretic characterization. *Dev. Biol.* **75**, 386-404.

Ogryzko, V. V., Schlitz, R. L., Russanova, V., Howard, B. H. and Nakatani, Y. (1996). The transcriptional coactivators p300 and CBP are histone acetyltransferases. *Cell* **87**, 953-959.

Oliva, R., Bazett-Jones, D., Mezquita, C. and Dixon, G. H. (1987). Factors affecting nucleosome disassembly by protamines in vitro. Histone hyperacetylation and chromatin structure, time dependence, and the size of the sperm nuclear proteins. *J. Biol. Chem.* **262**, 17016-17025.

Perreault, S. D. (1992). Chromatin remodeling in mammalian zygotes. *Mut. Res.* **296**, 43-55.

Perry, C. A., Allis, C.D. and Annunziato, A. T. (1993). Parental nucleosomes segregated to newly replicated chromatin are underacetylated relative to those assembled de novo. *Biochemistry* **32**, 13615-13623.

Philpott, A. and Leno, G. H. (1992). Nucleoplasmin remodels sperm chromatin in *Xenopus* egg extracts. *Cell* **69**, 759-767.

Ram, P.T. and Schultz, R. M. (1993). Reporter gene expression in G_2 of the 1-cell mouse embryo. *Dev. Biol.* **156**, 552-556.

Rundlett, S. E., Carmen, A. A., Kobayashi, R., Bavykin, S., Turner, B. M. and Grunstein, M. (1996). HDA1 and RPD3 are members of distinct yeast histone deacetylase complexes that regulate silencing and transcription. *Proc. Natl. Acad. Sci. USA* **93**, 14503-14508.

Segil, N., Guermah, M., Hoffmann, A., Roeder, R. G. and Heintz, N. (1996). Mitotic regulation of TFIID: inhibition of activator-dependent transcription and changes in subcellular localization. *Genes Dev.* **10**, 2389-2400.

Solter, D. (1988). Differential imprinting and expression of maternal and paternal genomes. *Annu. Rev. Genet.* **22**, 127-146.

Surrallés, J., Jeppesen, P., Morrison, H. and Natarajan, A. T. (1996). Analysis of loss of inactive X chromosomes in interphase cells. *Am. J. Hum. Genet.* **59**, 1091-1096.

Thompson, E. M., Legouy, E., Christians, E. and Renard, J. P. (1995). Progressive maturation of chromatin structure regulates *HSP70.1* gene expression in the preimplantation mouse embryo. *Development* **121**, 3425-3437.

Turner, B. M. and Fellows, G. (1989). Specific antibodies reveal ordered and cell-cycle-related use of histone-H4 acetylation sites in mammalian cells. *Eur. J. Biochem.* **179**, 131-139.

Vettese-Dadey, M., Grant, P. A., Hebbes, T. R., Crane-Robinson, C., Allis, C. D. and Workman, J. L. (1996). Acetylation of histone H4 plays a primary role in enhancing transcription factor binding to nucleosomal DNA in vitro. *EMBO J.* **15**, 2508-2518.

Wassarman, P. M. and Mrozak, S. C. (1981). Program of early development in the mammal: synthesis and intracellular migration of histone H4 during oogenesis in the mouse. *Dev. Biol.* **84**, 364-371.

Wiekowski, M., Miranda, M. and DePamphilis, M. L. (1993). Requirements for promoter activity in mouse oocytes and embryos distinguish paternal pronuclei from maternal and zygotic nuclei. *Dev. Biol.* **159**, 366-378.

Wilmut, I., Schnieke, A. E., McWhir, J., Kind, A. J. and Campbell, K. H. S. (1997). Viable offspring derived from fetal and adult mammalian cells. *Nature* **385**, 810-813.

Worrad, D. M., Ram, P. T. and Schultz, R. M. (1994). Regulation of gene expression in the mouse oocyte and early preimplantation embryo: developmental changes in Sp1 and TATA box-binding protein, TBP. *Development* **120**, 2347-2357

Worrad, D. M., Turner, B. M. and Schultz, R. M. (1995). Temporally restricted spatial localization of acetylated isoforms of histone H4 and RNA polymerase II in the 2-cell mouse embryo. *Development* **121**, 2949-2959.

Yang, X.-J., Ogoryzko, V.V., Nishikawa, J., Howard, B. H. and Nakatani, Y. (1996). A p300/CBP-associated factor that competes with the adenoviral oncoprotein E1A. *Nature* **382**, 319-324.

Yoshida M., Kijima M., Akita, M. and Beppu, T. (1990). Potent and specific inhibition of mammalian histone deacetylase both in vivo and in vitro by Trichostatin A. *J. Biol. Chem.* **265,** 17174-17179.

(Accepted 6 September 1997)